

**$^{228}\text{Th}$  nuclear states fed in  $^{228}\text{Ac}$  decay**

J. Dalmasso, H. Maria, and G. Ardisson

*Laboratoire de Radiochimie, Faculté des Sciences, Université de Nice, F-06034 Nice Cedex, France*

(Received 6 February 1987)

The decay of radiochemically-separated  $^{228}\text{Ac}$  sources has been reinvestigated using high-resolution coaxial HPGe detectors and  $\gamma$ - $\gamma$  coincidence measurements. Energies and intensities of more than 240 photons were accurately measured, 80 of them for the first time. A  $^{228}\text{Th}$  level scheme, built on the bases of good energy fits and on  $\gamma$ - $\gamma$  coincidence data, involves 58 excited states, of which 17 are new, up to 2159 keV with spin  $0 \leq I \leq 6$ . Collective properties of low-energy states belonging to  $K^\pi=0^-, 2^+, 2^-$  bands are discussed in the framework of the Bohr-Mottelson model. Decay modes of a  $K^\pi=0^+$  excited band at 831.82 keV favor strong two octupole phonon  $K^\pi=0^-$  components. The  $K^\pi=1^-$  band is expected to have  $I=2$  and 3 members at 938.5 and 968.4 keV. Coriolis coupling calculations involving the four  $K^\pi=0^-, 1^-, 2^-,$  and  $3^-$  bands were carried out. Tentative  $K^\pi=2^+$  two-quasiparticle bands at 1638.23 and 1899.99 keV are discussed in terms of Nilsson orbitals.

**I. INTRODUCTION**

$^{228}\text{Th}$  is a moderately deformed nucleus whose level structure study would be an interesting test of the validity of the recent cluster model of Daley and Iachello<sup>1-3</sup> in this mass region. Unfortunately, very few nuclear reactions are available to populate the  $^{228}\text{Th}$  nuclear levels because of the lack of a stable target in the vicinity of this nucleus. Two-neutron transfer reactions<sup>4</sup> have been used in the past to feed low-spin ( $0 \leq I \leq 2$ ) states in  $^{228}\text{Th}$  and a strong population of the  $K^\pi=0^+$  excited band was observed in the  $^{230}\text{Th}(p,t)$  reaction. More recently, Hardt *et al.*<sup>5</sup> used the  $\text{Th}(\alpha, \alpha'2n\gamma)$  reaction to populate high-spin levels of the  $^{228}\text{Th}$  ground-state band up to  $I=14$ , and the first octupole band,  $K^\pi=0^-$ , up to spin  $I=13$ . Otherwise, radioactive decay studies have been performed which feed  $^{228}\text{Th}$  levels up to 2200 keV. The  $^{228}\text{Pa}$  decay ( $I^\pi=3^+$ ) has been studied by  $\gamma$ -ray spectroscopy, electron spectroscopy, and coincidence measurements by Kurcewicz *et al.*<sup>6</sup> As concerns  $^{228}\text{Ac}$  decay, which also possesses  $I^\pi=3^+$ , several fragmentary reports were published by Herment *et al.*<sup>7,8</sup> and Dalmasso *et al.*,<sup>9-11</sup> both using Ge(Li) detectors and  $\gamma$ - $\gamma$  coincidence data. Finally, as noticed by the Nuclear Data Group,<sup>12</sup> several discrepancies remained, and the level scheme was not complete.

We intended to resolve some of these inconsistencies, working with radiochemically-separated  $^{228}\text{Ac}$  sources (instead of  $^{228}\text{Ra}$  equilibrium sources as in Refs. 9 and 10) measured with higher-efficiency HPGe detectors. A brief report concerning the  $^{228}\text{Ac}$   $\gamma$ -ray spectrum has been published elsewhere.<sup>13</sup>

**II. EXPERIMENTAL DETAILS****A. Source preparation**

The radiochemical separation procedure for  $^{228}\text{Ac}$  sources has been described elsewhere.<sup>13</sup> Briefly, a  $^{228}\text{Ra}$

source was isolated, carrier-free, from its  $^{232}\text{Th}$  parent by liquid extraction of 1 kg of thorium nitrate in a 40% tributylphosphate (TBP) solution in kerosene. The aqueous phase, containing  $^{228}\text{Ra}$ , was then diluted to 8.5M in  $\text{HClO}_4$  and passed through a 2 cm<sup>3</sup> volume DOWEX

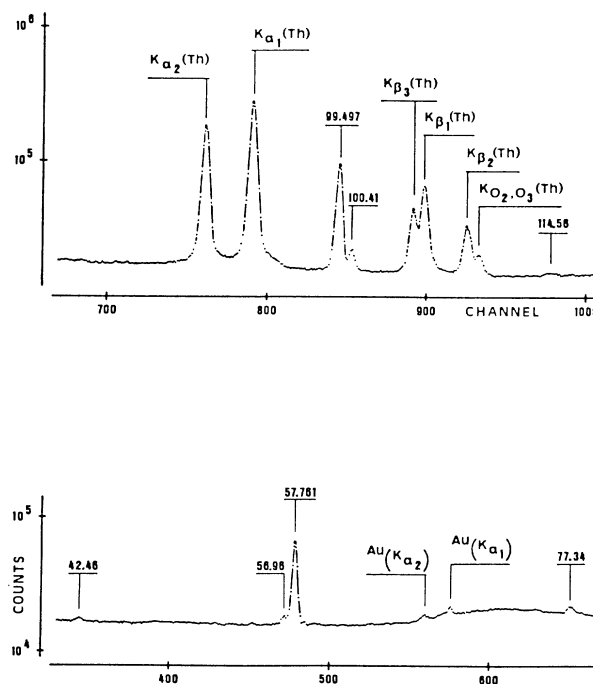


FIG. 1. Low energy  $\gamma$ -ray spectrum of  $^{228}\text{Ac}$  measured with the LEPS detector. Energies are in keV; the energy dispersion is 0.114 keV/channel. Au  $K\alpha$  lines are due to induced fluorescence in the gold contacts of the detector.

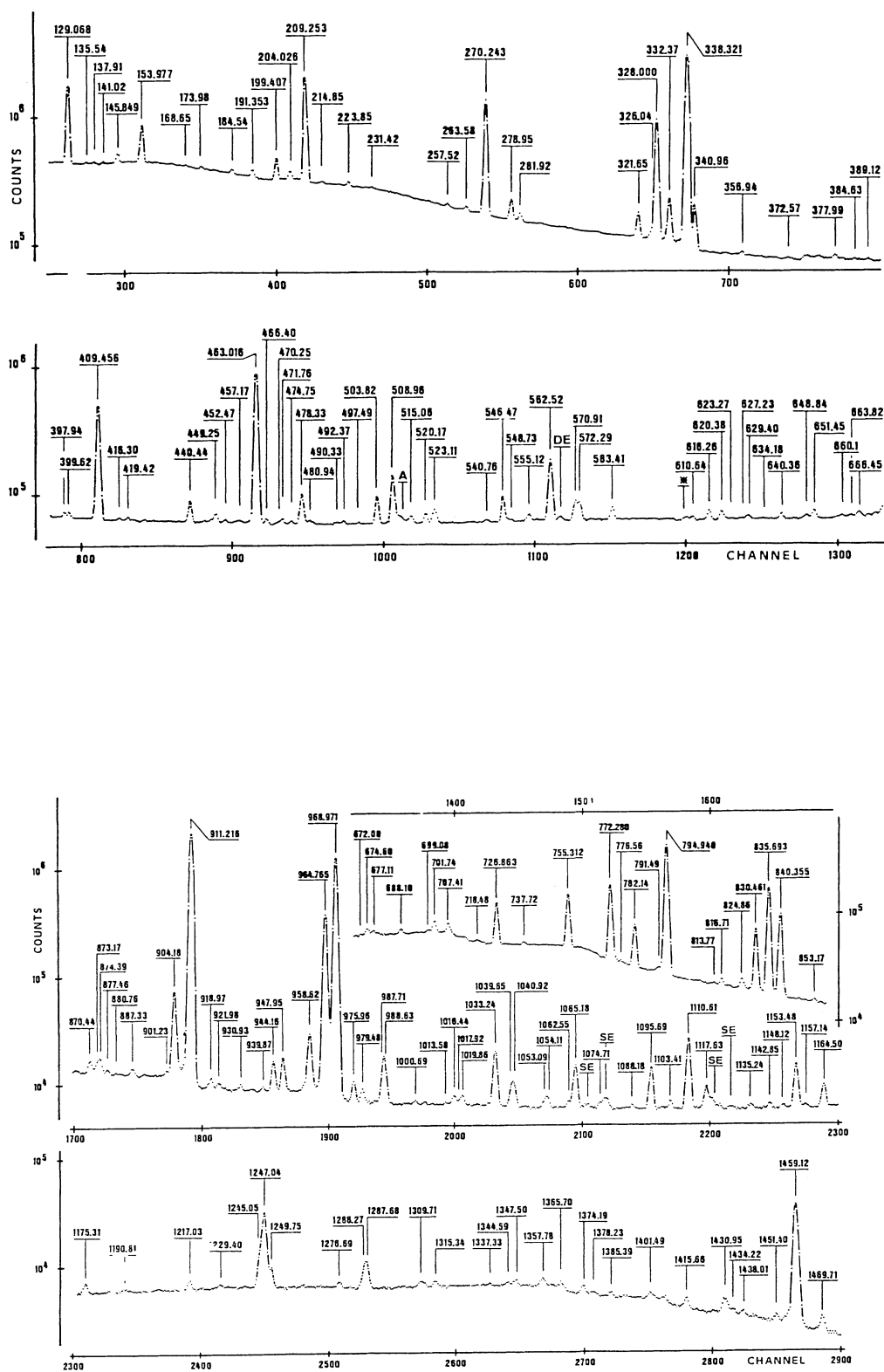


FIG. 2.  $\gamma$ -ray spectrum of  $^{228}\text{Ac}$  ( $120 \text{ keV} < E_\gamma < 2100 \text{ keV}$ ) taken with a 17% HPGe detector. Energies are in keV. The energy dispersion is 0.511 keV/channel. An asterisk denotes  $\gamma$  lines from background natural series ( $^{212}\text{Po}$ ,  $^{214}\text{Po}$ ). Counting time, 187 ks. A denotes annihilation line; SE, single escape; DE, double escape.

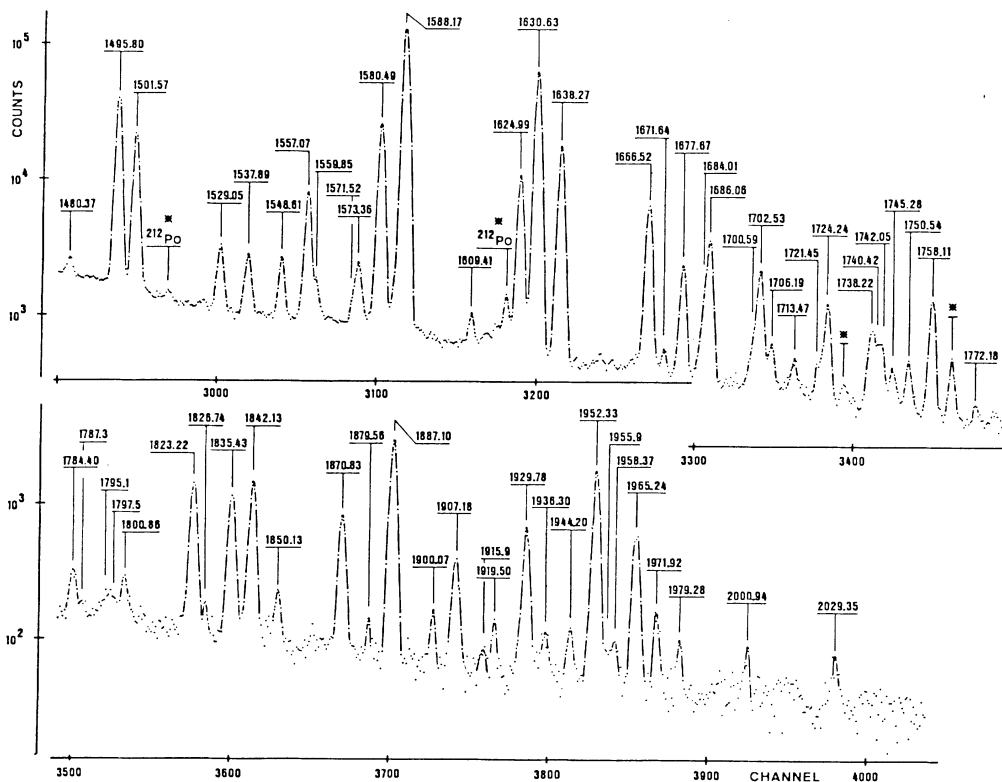


FIG. 2. (Continued).

50WX-8 cation exchange column. Under these conditions,  $^{228}\text{Ra}$  is not sorbed and  $^{228}\text{Ac}$  remains on the column from which it can be eluted using a 6M  $\text{HNO}_3$  solution. The first three column volumes, containing the  $^{212}\text{Bi}$  activity, were discarded and the next fractions contained almost pure  $^{228}\text{Ac}$ . Final sources were obtained by coprecipitation of  $^{228}\text{Ac}$  with  $\text{Fe}(\text{OH})_3$  as carrier. After a 10 h growth period, the  $^{228}\text{Ra}$  eluate was again passed through the cation column to obtain a new  $^{228}\text{Ac}$  source.

### B. Spectrometers

$\gamma$ -ray spectra were measured mainly with a coaxial HPGe detector (EG&G Ortec) having a relative efficiency of 17% and a peak to Compton ratio of 53:1. The energy resolution (FWHM) measured at 1.33 MeV was 1.85 keV. For low energy photons ( $X$  and  $\gamma$ ), the spectra were taken with a low-energy photon spectrometer (LEPS) detector (from EG&G Ortec) having an area of  $2\text{ cm}^2$  and a FWHM of 180 eV at the  $\text{Fe } K\alpha$   $X$  line. A 10% Ge(Li) detector (FWHM = 2.2 keV) was also used as a gating detector to perform  $\gamma$ - $\gamma$  coincidence experiments. The analysis systems typically used were 4096-channel (5400 Norland) and 8192-channel (918 ADCAM system, EG&G Ortec) analyzers coupled with a disk-based PDP 11/23 microcomputer.

## III. MEASUREMENTS AND RESULTS

### A. Singles spectra

Numerous  $\gamma$ -ray spectra following  $^{228}\text{Ac}$  decay were recorded with the different detectors described above. Each spectrum was obtained by accumulating counts from six or seven different sources counted for about 10 h. In order to identify summing peaks, different counting geometries were used by varying the source to detector distance between 5 and 15 cm. Precise  $\gamma$  energies of  $^{228}\text{Ac}$  main photopeaks were determined by simultaneous runs with standard sources such as  $^{152}\text{Eu}$ ,  $^{182}\text{Ta}$ ,  $^{207}\text{Bi}$ ,  $^{60}\text{Co}$ , and  $^{144}\text{Ce}$ - $^{144}\text{Pr}$ . Figure 1 shows the low energy part of the  $^{228}\text{Ac}$  ( $X + \gamma$ )-ray spectrum measured with the LEPS using an energy dispersion of 0.11 keV/channel. Figure 2 displays the medium and high energy  $\gamma$ -ray spectrum obtained with the 17% HPGe detector using seven different sources. The radiochemical purity of the  $^{228}\text{Ac}$  sources was confirmed by the absence in the spectra of the 238.58-keV  $\gamma$  line which belongs to the  $^{212}\text{Pb}$  decay.

Table I summarizes the energy and intensity values of the  $^{228}\text{Ac}$   $\gamma$  lines found in this work, together with their placements in the  $^{228}\text{Th}$  level scheme (Fig. 4 and Sec. IV). Our values are in good agreement with the Nuclear Data Sheets<sup>12</sup> compiled list which includes both the Herment *et al.*<sup>7,8</sup> and Dalmasso *et al.*<sup>9,10</sup> results, and also with the more precise energy values published by Helmer<sup>14</sup> (within 0.1 keV maximum deviation). From this table, it appears that 240  $\gamma$  transitions are attributed to  $^{228}\text{Ac}$   $\beta$  decay, of which 80 are new.

TABLE I. Gamma ray energies and intensities in the  $^{228}\text{Ac}$   $\beta$  decay. The numbers in parentheses denote the uncertainties ( $1\sigma$ ) in the last digits of the energies and intensities values. The relative intensities have been normalized to 1000 photons for the 911.216 keV  $\gamma$  line.

$E_\gamma$ (keV)	$I_\gamma$	Initial level	$K$	$I^\pi$	Final level	$K$	$I^\pi$
42.46(5)	0.35(10)	1688.38	2	$3^+$	1645.9	(3)	
56.96(5)	0.75(15)						
57.761(6)	16.9(17)	57.76	0	$2^+$	0	0	$0^+$
77.34(3)	0.99(20)	1168.36	2	$3^-$	1091.00	2	$4^+$
99.497(6)	44(5)	1531.48		$3^+$	1431.98	3	$3^+$
100.41(3)	3.6(5)	1122.94	2	$2^-$	1022.52	2	$3^+$
114.56(7)	0.38(8)	1645.89	(3)		1531.48		$3^+$
129.068(6)	101(10)	186.83	0	$4^+$	57.76	0	$2^+$
135.54(5)	0.68(14)	1226.55	2	$4^-$	1091.00	2	$4^+$
137.91(5)	0.91(18)						
141.02(3)	1.95(30)	519.20	0	$5^-$	378.18	0	$6^+$
145.849(10)	5.9(6)	1168.36	2	$3^-$	1022.52	2	$3^+$
153.977(10)	30(3)	1122.94	2	$2^-$	968.97	2	$2^+$
168.65(10)	0.50(10)	1344.03		3	1175.4		$2^+$
173.98(10)	1.35(20)	1153.49	(2)	$2^+$	979.50		$2^+$
184.54(2)	2.7(3)	1153.49	(2)	$2^+$	968.97	2	$2^+$
191.353(10)	5.0(5)	378.18	0	$6^+$	186.83	0	$4^+$
199.407(10)	12.2(12)	1168.36	2	$3^-$	968.97	2	$2^+$
204.026(10)	5.1(5)	1226.55	2	$4^-$	1022.52	2	$3^+$
209.253(6)	161(12)	396.08	0	$3^-$	186.83	0	$4^+$
214.85(10)	1.14(17)	2010.17	2	$4^+$	1795.90		$(4^+, 3^-)$
223.85(10)	2.1(2)	1450.29	3	$3^-$	1226.55	2	$4^-$
231.42(10)	0.96(14)	1175.41		$2^+$	944.18		$2^+$
257.52(10)	1.15(12)	1431.98	3	$3^+$	1174.2		$5^+$
263.58(10)	1.55(16)	1431.98	3	$3^+$	1168.36	2	$3^-$
270.243(7)	128(9)	328.00	0	$1^-$	57.76	0	$2^+$
278.95(5)	7.4(5)	1153.49		$2^+$	874.4	0	$2^+$
281.92(5)	2.4(2)	1450.29	3	$3^-$	1168.36	2	$3^-$
321.65(5)	8.4(6)	1153.49		$2^+$	831.82	0	$0^+$
326.04(20)	1.29(20)	1758.24		$(3,4)^+$	1431.98	3	$3^+$
328.000(6)	115(6)	328.001	0	$1^-$	0	0	$0^+$
332.37(5)	16.2(11)	519.20	0	$5^-$	186.83	0	$4^+$
338.321(6)	423(21)	396.08	0	$3^-$	57.76	0	$2^+$
340.96(5)	12.7(9)	1431.98	3	$3^+$	1091.00	2	$4^+$
356.94(10)	0.66(7)	1531.48		$3^+$	1174.2		$5^+$
372.57(20)	0.26(6)	2010.17	2	$4^+$	1638.23	2	$2^+$
377.99(10)	0.95(10)	1531.48		$3^+$	1153.49	(2)	$2^+$
384.63(20)	0.26(6)	2022.73		$2^+$	1638.23	2	$2^+$
389.12(15)	0.40(6)	1928.53		$(3,4)^+$	1539.13		$(2,3)$
397.94(10)	1.06(10)	1937.17		$(3,4)^+$	1539.13		$(2,3)$
399.62(10)	1.14(11)	1743.84		3	1344.03		$3^-$
409.456(10)	74(4)	1431.98	3	$3^+$	1022.52	2	$3^+$
416.30(20)	0.51(8)	1539.13		$(2,3)$	1122.94	2	$2^-$
419.42(10)	0.80(12)	1645.89		(3)	1226.55	2	$4^-$
440.44(5)	4.7(3)	1531.48		$3^+$	1091.00	2	$4^+$
449.25(10)	1.85(20)	968.38	(1)	$3^-$	519.20	0	$5^-$
452.47(10)	0.60(20)	1431.98	3	$3^+$	979.50		$2^+$
457.17(15)	0.58(9)	1683.71		$(3,4)^-$	1226.55	2	$4^-$
463.016(10)	165(8)	1431.98	3	$3^+$	968.97	2	$2^+$
466.40(10)	1.11(11)						
470.25(20)	0.50(10)	1638.23	2	$2^+$	1168.36	2	$3^-$
471.76(15)	1.26(12)	1415.92		$2^+$	944.18		$2^+$
474.75(10)	0.85(13)	1643.21		$(2,3)$	1168.36	2	$3^-$
478.33(5)	8.1(6)	874.4	0	$2^+$	396.08	0	$3^-$
480.94(20)	0.90(18)	1450.29	3	$3^-$	968.97	2	$2^+$
490.33(15)	0.43(9)	1906.78		$(2^+, 1^-)$	1415.92		$2^+$
492.37(10)	0.91(9)	1645.89		(3)	1153.49	(2)	$2^+$

TABLE I. (Continued).

$E_\gamma$ (keV)	$I_\gamma$	Initial level	$K$	$I^\pi$	Final level	$K$	$I^\pi$
497.49(15)	0.23(7)	1724.29		2 <sup>+</sup>	1226.55	2	4 <sup>-</sup>
503.82(5)	7.0(5)	831.82	0	0 <sup>+</sup>	328.001	0	1 <sup>-</sup>
508.96(5)	17.6(18)	1531.48		3 <sup>+</sup>	1022.52	2	3 <sup>+</sup>
515.06(10)	1.88(19)	1638.23	2	2 <sup>+</sup>	1122.94	2	2 <sup>-</sup>
520.17(5)	2.6(2)	1643.21		(2,3)	1122.94	2	2 <sup>-</sup>
523.11(5)	4.0(3)	1645.89		3	1122.94	2	2 <sup>-</sup>
540.76(10)	1.01(10)	1059.94		(4 <sup>+</sup> , 3 <sup>-</sup> )	519.20	0	5 <sup>-</sup>
546.47(5)	7.8(5)	874.4	0	2 <sup>+</sup>	328.00	0	1 <sup>-</sup>
548.73(15)	0.89(13)	1724.29		2 <sup>+</sup>	1175.41		2 <sup>+</sup>
555.12(10)	1.78(18)	1645.89		(3)	1091.00	2	4 <sup>+</sup>
562.52(3)	31(2)	1531.48		3 <sup>+</sup>	968.97	2	2 <sup>+</sup>
570.91(10)	6.3(6)	1539.13		(2,3)	968.97	2	2 <sup>+</sup>
572.29(10)	5.8(6)	968.38		3 <sup>-</sup>	396.08	0	3 <sup>-</sup>
583.41(5)	4.3(4)	979.50		2 <sup>+</sup>	396.08	0	3 <sup>-</sup>
610.64(10)	0.89(18)	938.5	(1)	2 <sup>-</sup>	328.00	0	1 <sup>-</sup>
616.26(10)	3.1(2)	944.18		2 <sup>+</sup>	328.00	0	1 <sup>-</sup>
620.38(5)	3.1(2)	1016.42		2 <sup>+</sup>	396.08	0	3 <sup>-</sup>
623.27(20)	0.43(10)	1645.89		(3)	1022.52	2	3 <sup>+</sup>
627.23(20)	0.54(11)	1643.21		(2,3)	1016.42		2 <sup>+</sup>
629.40(5)	1.74(18)	1645.89		(3)	1016.42		2 <sup>+</sup>
634.18(10)	0.41(8)						
640.36(5)	2.1(2)	968.38	(1)	3 <sup>-</sup>	328.00	0	1 <sup>-</sup>
648.84(10)	1.55(15)	1168.36	2	3 <sup>-</sup>	519.20	0	5 <sup>-</sup>
651.45(5)	3.5(3)	979.50		2 <sup>+</sup>	328.00	0	1 <sup>-</sup>
660.1(3)	~0.2	1682.69		(3,4) <sup>+</sup>	1022.52	2	3 <sup>+</sup>
663.82(10)	1.09(22)	1059.94		(4 <sup>+</sup> , 3 <sup>-</sup> )	396.082	0	3 <sup>-</sup>
666.45(10)	2.4(2)	1645.89		(3)	979.50		2 <sup>+</sup>
672.00(15)	1.00(30)	1683.71		(3,4) <sup>-</sup>	1016.42		2 <sup>+</sup>
674.60(10)	3.9(3)	1643.21		(2,3)	968.97	2	2 <sup>+</sup>
677.11(10)	2.4(2)	1645.89		(3)	968.97	2	2 <sup>+</sup>
688.10(5)	2.6(2)	874.4	0	2 <sup>+</sup>	186.83	0	2 <sup>+</sup>
699.08(15)	1.42(21)	1643.21		(2,3)	944.18		2 <sup>+</sup>
701.74(5)	6.7(4)	1724.29		2 <sup>+</sup>	1022.52	2	3 <sup>+</sup>
707.41(5)	6.0(6)	1226.55	2	4 <sup>-</sup>	519.20	0	5 <sup>-</sup>
718.48(15)	0.72(14)	1944.85	2	3 <sup>+</sup>	1226.55	2	4 <sup>-</sup>
726.863(15)	24(3)	1122.94	2	2 <sup>-</sup>	396.08	0	3 <sup>-</sup>
737.72(5)	1.43(14)	1760.25	2	4 <sup>+</sup>	1022.52	2	3 <sup>+</sup>
755.312(15)	36(2)	1724.29		2 <sup>+</sup>	968.97	2	2 <sup>+</sup>
772.280(10)	56(3)	1168.36	2	3 <sup>-</sup>	396.08	0	3 <sup>-</sup>
774.1(2)	~2.3	831.82	0	0 <sup>+</sup>	57.76	0	2 <sup>+</sup>
776.56(10)	0.73(22)	1944.85	2	3 <sup>+</sup>	1168.36	2	3 <sup>-</sup>
782.14(5)	18.7(9)	968.97	2	2 <sup>+</sup>	186.83	0	4 <sup>+</sup>
791.49(25)	0.89(27)	1760.25	2	4 <sup>+</sup>	968.97	2	2 <sup>+</sup>
792.8	~3	979.50		2 <sup>+</sup>	186.83	0	2 <sup>+</sup>
794.940(10)	162(9)	1122.94	2	2 <sup>-</sup>	328.00	0	1 <sup>-</sup>
813.77(15)	0.27(6)	1688.38	2	3 <sup>+</sup>	874.4	0	2 <sup>+</sup>
816.71(10)	1.16(12)	874.4	0	2 <sup>+</sup>	57.76	0	2 <sup>+</sup>
824.86(10)	1.95(20)	1344.03		3 <sup>-</sup>	519.20	0	5 <sup>-</sup>
830.461(20)	21(1)	1226.55	2	4 <sup>-</sup>	396.08	0	3 <sup>-</sup>
835.693(20)	62(3)	1022.52	2	3 <sup>+</sup>	186.83	0	4 <sup>+</sup>
840.355(20)	33(2)	1168.36	2	3 <sup>-</sup>	328.00	0	1 <sup>-</sup>
853.17(10)	0.46(7)	1944.85	2	3 <sup>+</sup>	1091.00	2	4 <sup>+</sup>
870.44(5)	1.70(17)	1892.96		(3,4) <sup>+</sup>	1022.52	2	3 <sup>+</sup>
873.17(15)	1.20(24)	1059.94		(4 <sup>+</sup> , 3 <sup>-</sup> )	186.83	0	4 <sup>+</sup>
874.39(15)	1.84(40)	874.4	0	2 <sup>+</sup>	0	0	0 <sup>+</sup>
877.46(10)	0.53(10)	1899.99	2	2 <sup>+</sup>	1022.52	2	3 <sup>+</sup>
880.76(10)	0.24(7)	938.5	(1)	2 <sup>-</sup>	57.76	0	2 <sup>+</sup>
887.33(10)	1.06(10)	2010.17	2	4 <sup>+</sup>	1122.94	2	2 <sup>-</sup>
901.23(15)	0.63(13)	1297.3	2	5 <sup>-</sup>	396.08	0	3 <sup>-</sup>

TABLE I. (Continued).

$E_\gamma$ (keV)	$I_\gamma$	Initial level	$K$	$I^\pi$	Final level	$K$	$I^\pi$
904.18(5)	28(2)	1091.00	2	4 <sup>+</sup>	186.829	0	4 <sup>+</sup>
911.216(10)	1000	968.97	2	2 <sup>+</sup>	57.76	0	2 <sup>+</sup>
918.97(10)	1.05(10)	2010.17	2	4 <sup>+</sup>	1091.00	2	4 <sup>+</sup>
921.98(10)	0.57(8)	979.50		2 <sup>+</sup>	57.76	0	2 <sup>+</sup>
930.93(10)	0.48(7)	1450.29	3	3 <sup>-</sup>	519.20	0	5 <sup>-</sup>
939.87(15)	0.34(10)	2029.6		(2 <sup>+</sup> )	1091.00	2	4 <sup>+</sup>
944.16(5)	3.7(3)	944.18		2 <sup>+</sup>	0	0	0 <sup>+</sup>
947.95(5)	4.1(3)	1344.03		3 <sup>-</sup>	396.08	0	3 <sup>-</sup>
958.62(5)	11.3(8)	1016.42		2 <sup>+</sup>	57.76	0	2 <sup>+</sup>
964.765(10)	194(10)	1022.52	2	3 <sup>+</sup>	57.76	0	2 <sup>+</sup>
968.971(10)	614(30)	968.97	2	2 <sup>+</sup>	0	0	0 <sup>+</sup>
975.96(5)	1.92(19)	1944.85	2	3 <sup>+</sup>	968.97	2	2 <sup>+</sup>
979.48(10)	1.02(10)	979.50		2 <sup>+</sup>	0	0	0 <sup>+</sup>
987.71(20)	3.0(5)	1174.2		5 <sup>+</sup>	186.83	0	4 <sup>+</sup>
988.63(20)	3.0(5)	1175.41		2 <sup>+</sup>	186.83	0	4 <sup>+</sup>
1000.69(15)	0.2	1944.85	2	3 <sup>+</sup>	944.18		2 <sup>+</sup>
1013.58(20)	0.18(5)	2029.6		(2 <sup>+</sup> )	1016.42		2 <sup>+</sup>
1016.44(15)	0.72(11)	1016.42		2 <sup>+</sup>	0	0	0 <sup>+</sup>
		1344.03		3 <sup>-</sup>	328.00	0	1 <sup>-</sup>
1017.92(20)	0.22(5)	1987.61		4 <sup>+</sup>	968.97	2	2 <sup>+</sup>
1019.86(10)	0.81(16)	1415.92		2 <sup>+</sup>	396.08	0	3 <sup>-</sup>
1033.24(2)	7.8(5)	1091.00	2	4 <sup>+</sup>	57.76	0	2 <sup>+</sup>
1039.65(15)	1.73(35)	1226.55	2	4 <sup>-</sup>	186.83	0	4 <sup>+</sup>
1040.92(15)	1.73(35)	2010.17	2	4 <sup>+</sup>	968.97	2	2 <sup>+</sup>
1053.09(20)	0.52(15)	2022.73		2 <sup>+</sup>	968.97	2	2 <sup>+</sup>
1054.11(20)	0.70(21)	1450.29	3	3 <sup>-</sup>	396.08	0	3 <sup>-</sup>
1062.55(15)	0.40(12)	1937.17		(3,4) <sup>+</sup>	874.4	0	2 <sup>+</sup>
1065.18(5)	5.1(4)	1122.94	2	2 <sup>-</sup>	57.76	0	2 <sup>+</sup>
1074.71(15)	0.39(12)	1906.78		(2 <sup>+</sup> , 1 <sup>-</sup> )	831.82	0	0 <sup>+</sup>
1088.18(15)	0.23(5)	1415.92		2 <sup>+</sup>	328.00	0	1 <sup>-</sup>
1095.69(5)	5.0(4)	1153.49	(2)	2 <sup>+</sup>	57.76	0	2 <sup>+</sup>
1103.41(10)	0.58(9)	1431.98	3	3 <sup>+</sup>	328.00	0	1 <sup>-</sup>
1110.61(5)	11.8(8)	1168.36	2	3 <sup>-</sup>	57.76	0	2 <sup>+</sup>
1117.63(10)	2.1(3)	1175.41		2 <sup>+</sup>	57.76	0	2 <sup>+</sup>
1135.24(15)	0.38(6)	1531.48		3 <sup>+</sup>	396.08	0	3 <sup>-</sup>
1142.85(15)	0.40(8)	1539.13		(2,3)	396.08	0	3 <sup>-</sup>
1148.12(15)	0.23(5)	2022.73		2 <sup>+</sup>	874.4	0	2 <sup>+</sup>
1153.48(5)	5.4(4)	1153.49	(2)	2 <sup>+</sup>	0	0	0 <sup>+</sup>
1157.14(15)	0.27(5)	1344.03		3 <sup>-</sup>	186.83	0	4 <sup>+</sup>
1164.50(8)	2.5(2)	1683.71		(3,4) <sup>+</sup>	519.20	0	5 <sup>-</sup>
1175.31(10)	0.93(13)	1175.41		2 <sup>+</sup>	0	0	0 <sup>+</sup>
1190.81(20)	0.24(6)	2022.73		2 <sup>+</sup>	831.82	0	0 <sup>+</sup>
1217.03(10)	0.82(12)	1735.62		4 <sup>+</sup>	519.20	0	5 <sup>-</sup>
1229.40(15)	0.29(9)	1415.92		2 <sup>+</sup>	186.83	0	4 <sup>+</sup>
1245.05(20)	3.7(7)	1431.98	3	3 <sup>+</sup>	186.83	0	4 <sup>+</sup>
1247.04(5)	18.5(9)	1643.21		(2,3)	396.08	0	3 <sup>-</sup>
1249.75(15)	2.4(2)	1645.89		(3)	396.08	0	3 <sup>-</sup>
1276.69(10)	0.54(11)	1795.90		(4 <sup>+</sup> , 3 <sup>-</sup> )	519.20	0	5 <sup>-</sup>
1286.27(20)	1.93(38)	1344.03		3 <sup>-</sup>	57.76	0	2 <sup>+</sup>
1287.68(20)	3.1(6)	1682.69		(3,4) <sup>+</sup>	396.08	0	3 <sup>-</sup>
1309.71(20)	0.73(24)	1638.23	2	2 <sup>+</sup>	328.00	0	1 <sup>-</sup>
1315.34(10)	0.57(11)	1643.21		(2,3)	328.00	0	1 <sup>-</sup>
1337.33(20)	0.19(6)						
1344.59(15)	0.35(7)	1531.48		3 <sup>+</sup>	186.83	0	4 <sup>+</sup>
1347.50(15)	0.60(12)	1743.84		3	396.08	0	3 <sup>-</sup>
1357.78(15)	0.79(16)	1735.62		4 <sup>+</sup>	378.18	0	6 <sup>+</sup>
1365.70(15)	0.53(11)						
1374.19(10)	0.53(15)	1431.98	3	3 <sup>+</sup>	57.76	0	2 <sup>+</sup>
1378.23(10)	0.23(7)						

TABLE I. (Continued).

$E_\gamma$ (keV)	$I_\gamma$	Initial level	$K$	$I^\pi$	Final level	$K$	$I^\pi$
1385.39(10)	0.41(8)						
1401.49(10)	0.47(10)	1797.65		(2 <sup>+</sup> , 1 <sup>-</sup> )	396.08	0	3 <sup>-</sup>
1415.66(10)	0.83(16)	1743.84		3	328.00	0	1 <sup>-</sup>
1430.95(10)	1.36(27)	1617.74		(3,4) <sup>+</sup>	186.83	0	4 <sup>+</sup>
1434.22(15)	0.31(9)						
1438.01(10)	0.23(6)						
1451.40(15)	0.41(8)	1638.23	2	2 <sup>+</sup>	186.83	0	4 <sup>+</sup>
1459.12(5)	31(2)	1645.89		(3)	186.83	0	4 <sup>+</sup>
1469.71(15)	0.78(15)	1797.90		(2 <sup>+</sup> , 1 <sup>-</sup> )	328.00	0	1 <sup>-</sup>
1480.37(15)	0.63(12)						
1495.80(5)	35(2)	1682.69		(3,4) <sup>+</sup>	186.83	0	4 <sup>+</sup>
1501.57(5)	18.5(13)	1688.38	2	3 <sup>+</sup>	186.83	0	4 <sup>+</sup>
1529.05(10)	2.2(2)						
1537.89(10)	1.81(18)	1724.29		2 <sup>+</sup>	186.83	0	4 <sup>+</sup>
1548.61(10)	1.47(15)	1735.62		4 <sup>+</sup>	186.83	0	4 <sup>+</sup>
1557.07(5)	6.9(5)	1743.84		3	186.83	0	4 <sup>+</sup>
1559.85(20)	0.79(16)	1617.74		(3,4) <sup>+</sup>	57.76	0	2 <sup>+</sup>
1571.52(20)	0.22(6)	1758.24		(3,4) <sup>+</sup>	186.83	0	4 <sup>+</sup>
1573.36(10)	1.27(13)	1760.25	2	4 <sup>+</sup>	186.83	0	4 <sup>+</sup>
1580.49(5)	24(2)	1638.23	2	2 <sup>+</sup>	57.76	0	2 <sup>+</sup>
1588.17(5)	126(6)	1645.89		3	57.76	0	2 <sup>+</sup>
1609.41(15)	0.30(6)	1987.61		4 <sup>+</sup>	378.18	0	6 <sup>+</sup>
1624.99(5)	9.9(7)	1682.69		(3,4) <sup>+</sup>	57.76	0	2 <sup>+</sup>
1630.63(5)	64(4)	1688.38	2	3 <sup>+</sup>	57.76	0	2 <sup>+</sup>
1638.27(5)	18.2(13)	1638.23	2	2 <sup>+</sup>	0	0	0 <sup>+</sup>
1666.52(5)	6.9(5)	1724.29		2 <sup>+</sup>	57.76	0	2 <sup>+</sup>
1671.64(15)	0.16(5)						
1677.67(5)	2.1(2)	1735.62		4 <sup>+</sup>	57.76	0	2 <sup>+</sup>
1684.01(20)	0.57(18)						
1686.06(5)	3.7(3)	1743.84		3	57.76	0	2 <sup>+</sup>
1700.59(20)	0.39(9)	1758.24		(3,4) <sup>+</sup>	57.76	0	2 <sup>+</sup>
1702.53(10)	1.86(18)	1760.25	2	4 <sup>+</sup>	57.76	0	2 <sup>+</sup>
1706.19(10)	0.33(4)	1892.96		(3,4) <sup>+</sup>	186.83	0	4 <sup>+</sup>
1713.47(20)	0.21(4)	1899.99	2	2 <sup>+</sup>	186.83	0	4 <sup>+</sup>
1721.45(30)	0.22(7)						
1724.24(10)	1.12(11)	1724.29		2 <sup>+</sup>	0	0	0 <sup>+</sup>
1738.22(25)	0.68(14)	1795.90		(4 <sup>+</sup> , 3 <sup>-</sup> )	57.76	0	2 <sup>+</sup>
1740.42(30)	0.42(12)	1797.65		(2 <sup>+</sup> , 1 <sup>-</sup> )	57.76	0	2 <sup>+</sup>
1742.05(30)	0.31(9)	1928.53		(3,4) <sup>+</sup>	186.83	0	4 <sup>+</sup>
1745.28(20)	0.25(3)						
1750.54(20)	0.31(3)	1937.17		(3,4) <sup>+</sup>	186.83	0	4 <sup>+</sup>
1758.11(10)	1.34(13)	1944.85	2	3 <sup>+</sup>	186.83	0	4 <sup>+</sup>
1772.18(30)	0.07(2)	1958.7		2	186.83	0	4 <sup>+</sup>
1784.40(30)	0.23(4)						
1787.3(5)	0.05(2)						
1795.1(5)	0.08(3)	2123.1		(2 <sup>+</sup> , 3 <sup>-</sup> )	328.00	0	1 <sup>-</sup>
1797.5(5)	0.08(3)	1797.65		(2 <sup>+</sup> , 1 <sup>-</sup> )	0	0	0 <sup>+</sup>
1800.86(20)	0.17(3)	1987.61		4 <sup>+</sup>	186.83	0	4 <sup>+</sup>
1823.22(10)	1.70(17)	2010.17	2	4 <sup>+</sup>	186.83	0	4 <sup>+</sup>
1826.74(30)	0.08(3)	2013.6		(3,4) <sup>+</sup>	186.83	0	4 <sup>+</sup>
1835.43(10)	1.46(14)	1892.96		(3,4) <sup>+</sup>	57.76	0	2 <sup>+</sup>
1842.13(10)	1.62(16)	1899.99	2	2 <sup>+</sup>	57.76	0	2 <sup>+</sup>
1850.13(20)	0.17(3)	2037.0		(3,4) <sup>+</sup>	186.83	0	4 <sup>+</sup>
1870.83(10)	0.94(9)	1928.53		(3,4) <sup>+</sup>	57.76	0	2 <sup>+</sup>
1879.56(30)	0.05(2)	1937.17		(3,4) <sup>+</sup>	57.76	0	2 <sup>+</sup>
1887.10(5)	3.5(3)	1944.85	2	3 <sup>+</sup>	57.76	0	2 <sup>+</sup>
1900.07(20)	0.11(2)	1899.99	2	2 <sup>+</sup>	0	0	0 <sup>+</sup>
1907.18(20)	0.46(4)	1906.78		(2 <sup>+</sup> , 1 <sup>-</sup> )	0	0	0 <sup>+</sup>
1915.9(4)	0.03(1)						

TABLE I. (Continued).

$E_\gamma$ (keV)	$I_\gamma$	Initial level	$K$	$I^\pi$	Final level	$K$	$I^\pi$
1919.50(30)	0.08(2)						
1929.78(20)	0.77(8)	1987.61		$4^+$	57.76	0	$2^+$
1936.30(30)	0.08(2)	2123.1		$(2^+, 3^-)$	186.83	0	$4^+$
1944.20(20)	0.08(2)						
1952.33(15)	2.3(2)	2010.17	2	$4^+$	57.76	0	$2^+$
1955.9(5)	0.03(1)	2013.6		$(3, 4)^+$	57.76	0	$2^+$
1958.37(30)	0.06(2)	1958.7			0	0	$0^+$
1965.24(20)	0.79(7)	2022.73		$2^+$	57.76	0	$2^+$
1971.92(30)	0.14(3)	2029.6		$(2^+)$	57.76	0	$2^+$
1979.28(30)	0.07(2)	2037.0		$(3, 4)^+$	57.76	0	$2^+$
2000.94(50)	0.04(1)						
2029.35(50)	0.07(2)	2029.6		$(2^+)$	0	0	$0^+$

### B. $\gamma$ - $\gamma$ coincidence measurements

Some  $\gamma$ - $\gamma$  coincidence experiments have been performed using the 17% HPGe detector and the LEPS as gating detector. The coincidence circuit, involving two constant fraction timing analyzers, has been described

elsewhere.<sup>15</sup> For the medium energy gates, the 17% HPGe detector was used in conjunction with a 10% Ge(Li) detector. In order to avoid Compton contributions from high energy  $\gamma$  lines of the daughters of  $^{228}\text{Th}$ , most experiments were carried out with freshly-prepared  $^{228}\text{Ac}$  sources. Energy gates of 99, 129, 209, 270, 328, 332, 338, 341, 357, 409, 440, 449, 463, 478, 509, 511, 555, 572, 583, 688, 701, 707, 727, 772, 782, 793, 795, 830, 835, 873, 904, 911, 919, 964, 969, 987, 988, 1039, 1245, 1247, 1431, 1459, 1496, 1501, 1538, 1548, 1573, 1557

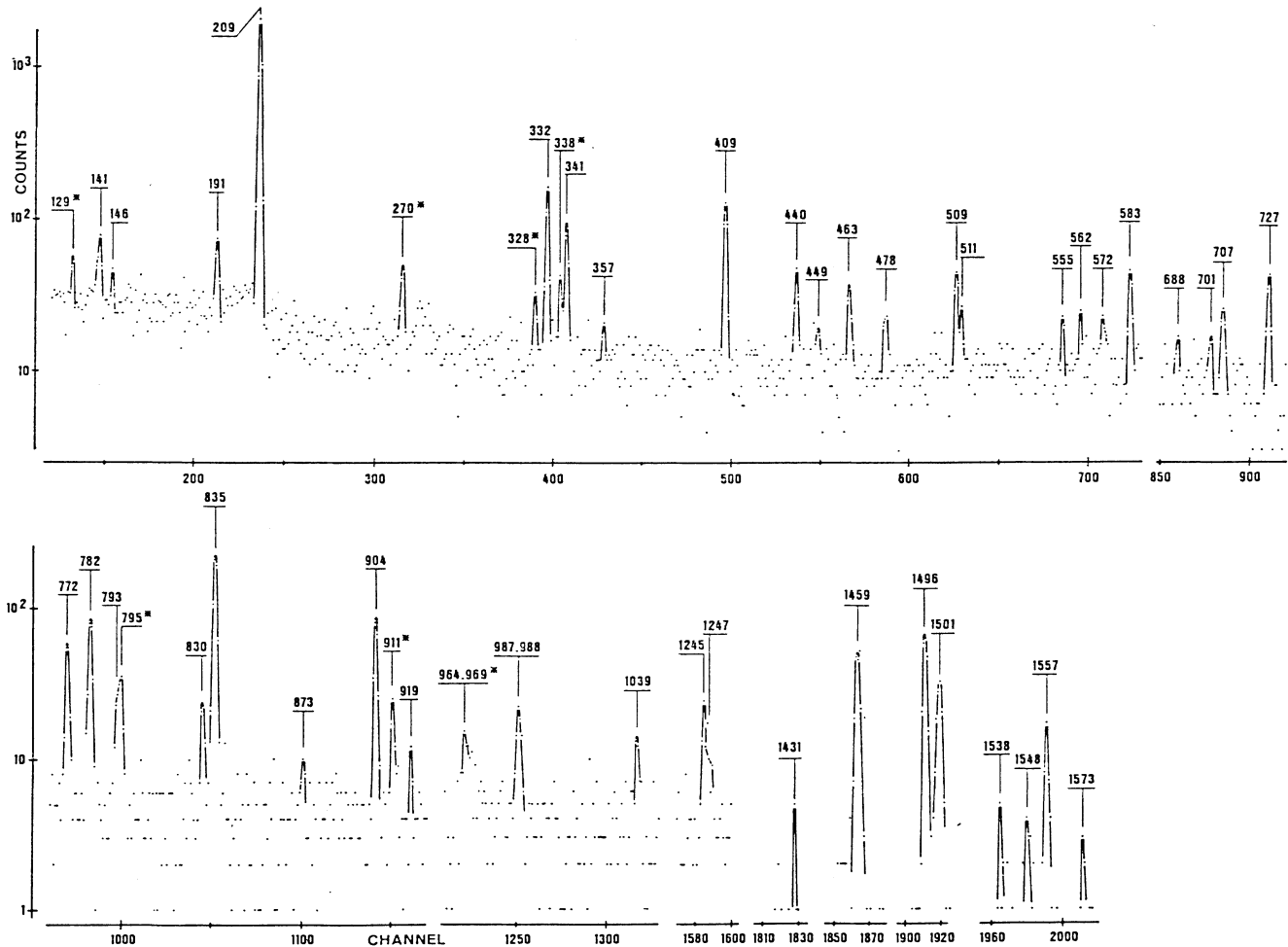


FIG. 3.  $^{228}\text{Ac}$   $\gamma$ - $\gamma$  coincidence spectrum taken with the 17% HPGe detector gated with a  $129 \pm 3$  keV window in the LEPS detector. Rounded values of the energies are given in keV. An asterisk denotes random coincidences.



TABLE II. Summary of the  $\gamma$ - $\gamma$  coincidence relationships. An asterisk denotes only seen in coincidence experiments.

Gate (keV)	Coincident transitions (keV)
99±3	263.6, 341.0, 409.4, 463.0, 835.7, 911.2, 964.8, 969.0, 1245.0, 1374.2
129±4	141.0, 145.8, 191.3, 209.2, 332.4, 341.0, 357.0, 409.4, 440.4, 449.2, 463.0, 478.3, 509.0, 555.1, 562.5, 572.3, 583.4, 688.1, 701.7, 707.4, 726.9, 772.3, 782.1, 792.8*, 830.5, 835.7, 873.2, 904.2, 919.0, 987.7, 988.6, 1039.6, 1245.0, 1247.04, 1430.9, 1459.1, 1495.8, 1501.6, 1537.9, 1548.6, 1557.0, 1573.4
209±4	281.9, 321.6, 503.8, 520.2, 523.1, 546.5, 610.6, 616.3, 640.4, 651.4, 794.9, 840.3
270±4	129.1, 278.9, 478.3, 572.3, 620.4, 663.8, 726.9, 772.3, 830.5, 901.2, 947.9, 1019.9, 1247.0, 1249.7, 1287.7
328±3	321.6, 503.8, 546.5, 616.3, 640.4, 794.9, 840.3
338±3	478.3, 572.3, 620.4, 726.9, 772.3, 830.5, 947.9, 1247.0, 1249.7, 1287.5
772±4	129.1, 209.2, 263.6, 281.9, 321.6, 338.3
911±7	77.3, 99.5, 129.1, 154.0, 184.5, 199.4, 341.0, 378.0, 440.4, 463.0, 555.1, 562.5, 570.9, 674.6, 677.1, 755.3, 791.5, 853.2, 919.0, 976.0, 1040.9

338, 772, and 911 keV were chosen in the Ge(Li) detector. Figure 3 displays a typical  $\gamma$ - $\gamma$  spectrum obtained with the 17% HPGe detector gated by the 129-keV window. Random coincidences, which were below 1% at the HPGe count rate ( $\sim 1000$  counts  $s^{-1}$ ), were not subtracted from this spectrum. Table II summarizes  $\gamma$ - $\gamma$  coincidence data obtained in these runs.

#### IV. THE $^{228}\text{Ac}$ DECAY SCHEME

A  $^{228}\text{Th}$  level scheme has been built on the bases of previous results of Dalmasso *et al.*,<sup>11</sup> Herment *et al.*,<sup>7</sup> and good energy fits using the Ritz principle with our improved energy values.  $\gamma$ - $\gamma$  coincidences also add strong arguments for placement of several  $\gamma$  lines. Figure 4 shows the  $^{228}\text{Th}$  level scheme deduced from these considerations. This level scheme accommodates 225  $\gamma$  lines (of the 240 measured ones) which represent more than 99.7% of the total  $\beta$  decay, among 58 excited levels, of which 17 are newly reported.

The  $\beta$  branches from  $^{228}\text{Ac}$  ( $KI^\pi = 33^+$ ) (Ref. 16) have been deduced from the ( $\gamma + ce$ ) intensity balances calcu-

lated at each level (ce denotes conversion electron).

Assuming no  $\beta$  decay to the  $^{228}\text{Th}$  ground state, the sum of each feeding has been normalized to  $100\beta$ . To include conversion electrons we have used the Herment data<sup>7</sup> for the strongest lines measured and the theoretical conversion coefficients<sup>17</sup> for the weakest lines; in particular for the 57.8-keV pure- $E2$   $\gamma$  line the theoretical  $\alpha_T = 157$  value was deduced from a double logarithmic interpolation from tables of Rösler *et al.*<sup>17</sup>

$\log ft$  values were calculated assuming  $Q_- = (2142 \pm 6)$  keV from the Wapstra and Audi mass adjustments,<sup>18</sup> a half-life  $T_{1/2} = (6.15 \pm 0.02)$  h (Ref. 19), and the matrix element  $f_0$  from the table of Gove and Martin.<sup>20</sup>

Table III gives the  $^{228}\text{Th}$  level energies deduced from this work, together with their percent  $\beta$  feeding and  $\log ft$ .

A normalization factor of 0.0287 was applied to convert the relative  $\gamma$  intensities of Table I in the absolute scale; this means that the 911 keV main transition was calculated to be  $(28.7 \pm 0.9)\%$  of the decays, which agrees very well with the absolute measurements of Schötzig and Debertain,<sup>21</sup> i.e.,  $I_\gamma(911) = 26.6(7)$ .

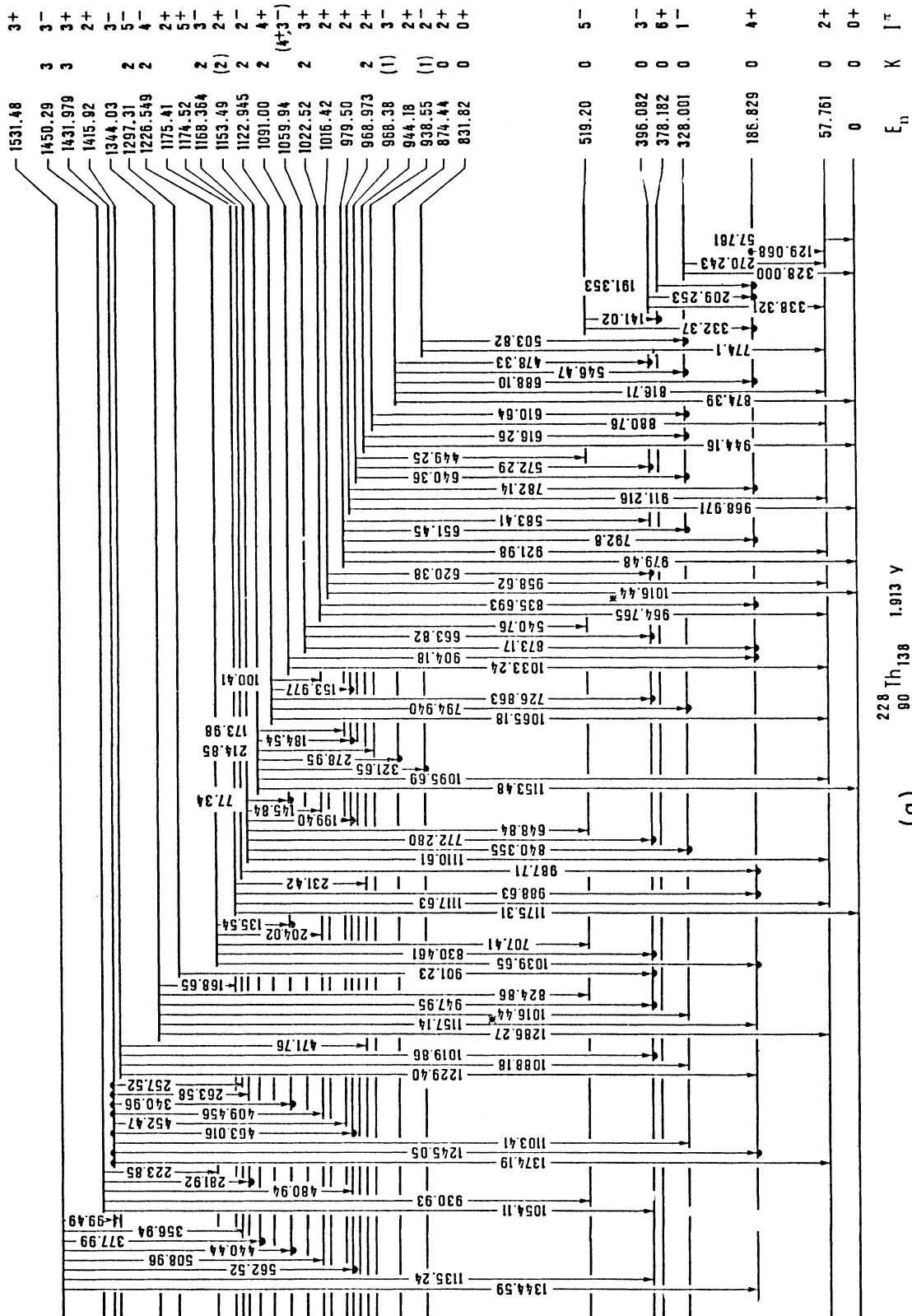


FIG. 4.  $^{228}\text{Th}$  levels fed in the  $^{228}\text{Ac}$  ( $KI^\pi = 33^+$ )  $\beta$  decay. The energies are in keV. Heavy dots indicate coincidence relationships (Table II). An asterisk denotes a  $\gamma$  line placed twice.  $\log ft$ 's and percent  $\beta$  feedings are shown in Table III.

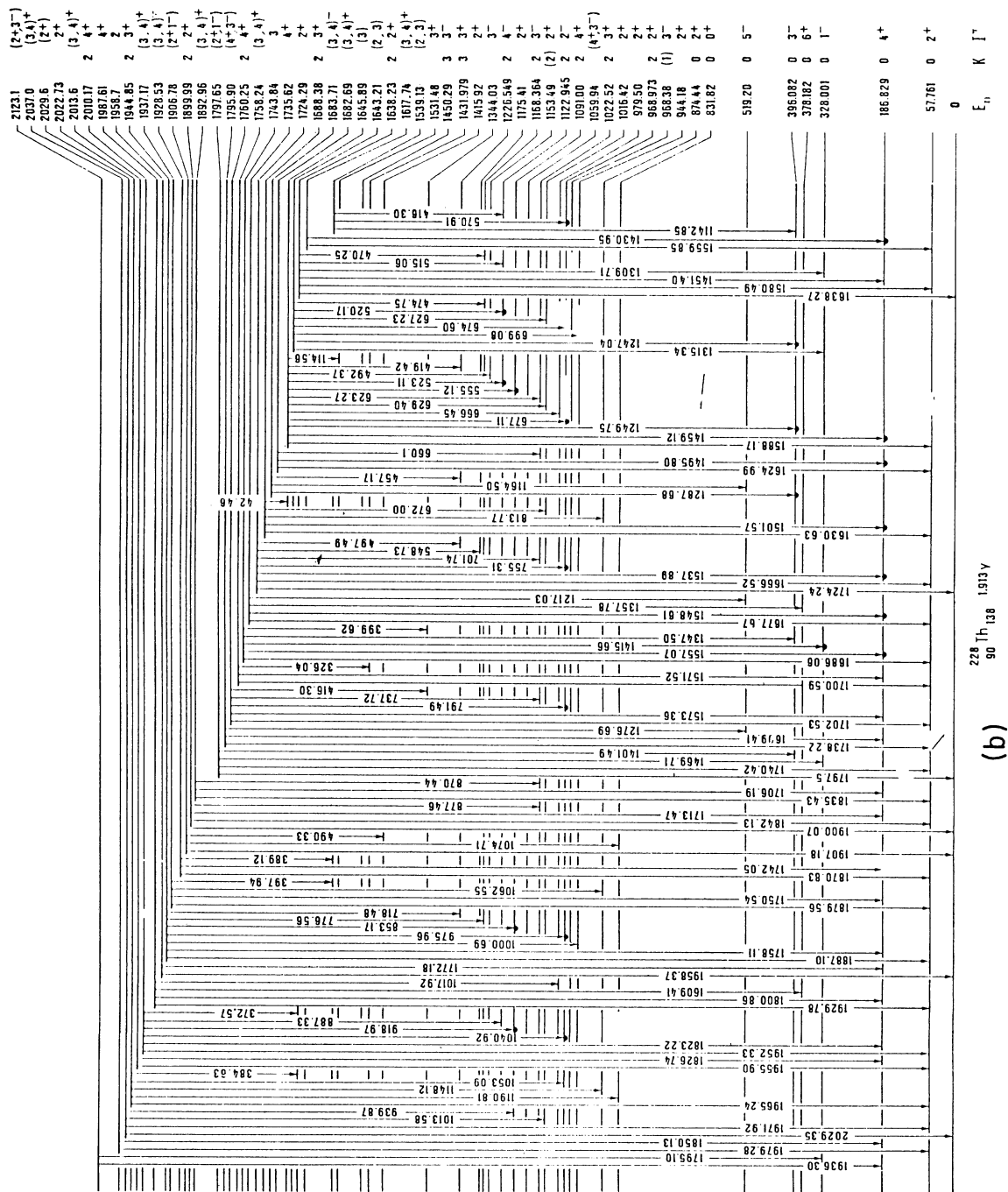


FIG. 4. (Continued).

TABLE III. Energies,  $KI^\pi$ ,  $\beta$  feedings, and  $\log ft$ 's for the  $^{228}\text{Th}$  excited states populated by  $^{228}\text{Ac}$   $\beta$  decay. Quantities in parentheses are the uncertainties ( $1\sigma$ ) in the last significant digits. An asterisk denotes the  $\log f^1 t$  values.  $\log ft$  uncertainties are less than 0.1 for  $\Delta I_\beta < 15\%$  and 0.2 otherwise.

Level energy (keV)	$K$	$I^\pi$	$I\beta^-$ (%)	$\log ft$
57.761(6)	0	2 <sup>+</sup>	3.1(30)	> 9.3
186.829(9)	0	4 <sup>+</sup>	1.6(8)	9.5
328.001(5)	0	1 <sup>-</sup>	0.74(40)	10.6*
378.182(13)	0	6 <sup>+</sup>	0	
396.082(7)	0	3 <sup>-</sup>	13.0(7)	8.4
519.20(3)	0	5 <sup>-</sup>	0.32(4)	10.7*
831.82(5)	0	0 <sup>+</sup>	0	
874.44(3)	0	2 <sup>+</sup>	0.16(3)	9.8
938.55(1)	(1)	2 <sup>-</sup>	0	
944.18(5)		2 <sup>+</sup>	0.025(7)	10.5
968.38(4)	(1)	3 <sup>-</sup>	0.31(2)	9.4
968.973(8)	2	2 <sup>+</sup>	38.1(18)	7.3
979.50(3)		2 <sup>+</sup>	0.15(5)	9.7
1016.42(4)		2 <sup>+</sup>	0.34(3)	9.3
1022.52(1)	2	3 <sup>+</sup>	3.47(20)	8.2
1059.94(7)		(4 <sup>+</sup> , 3 <sup>-</sup> )	0.095(5)	9.75
1091.00(2)	2	4 <sup>+</sup>	0.12(6)	9.6
1122.945(8)	2	2 <sup>-</sup>	6.4(3)	7.85
1153.49(2)	(2)	2 <sup>+</sup>	1.62(8)	8.4
1168.364(8)	2	3 <sup>-</sup>	3.7(2)	8.0
1174.52(2)	2	5 <sup>+</sup>	< 0.023	> 10.2
1175.41(6)		2 <sup>+</sup>	0.26(2)	9.15
1226.549(12)	2	4 <sup>-</sup>	0.76(4)	8.6
1297.31(2)	2	5 <sup>-</sup>	< 0.018	> 11.3*
1344.03(9)		3 <sup>-</sup>	0.24(2)	8.9
1415.92(7)		2 <sup>+</sup>	0.086(8)	9.2
1431.979(10)	3	3 <sup>+</sup>	1.54(70)	7.9
1450.29(4)	3	3 <sup>-</sup>	0.40(2)	8.5
1531.48(2)		3 <sup>+</sup>	8.6(5)	6.9
1539.13(6)		(2,3)	0.18(2)	8.6
1617.74(9)		(3,4) <sup>+</sup>	0.06(1)	8.9
1638.23(3)	2	2 <sup>+</sup>	1.3(1)	7.5
1643.21(3)		(2,3)	0.84(5)	7.7
1645.89(2)		(3)	5.0(2)	6.9
1682.69(4)		(3,4) <sup>+</sup>	1.3(1)	7.4
1683.71(6)		(3,4) <sup>-</sup>	0.18(1)	8.2
1688.38(3)	2	3 <sup>+</sup>	2.41(12)	7.1
1724.29(2)		2 <sup>+</sup>	1.62(15)	7.1
1735.62(4)		4 <sup>+</sup>	0.15(1)	8.1
1743.84(3)		3	0.38(2)	7.7
1758.24(12)		(3,4) <sup>+</sup>	0.082(12)	8.3
1760.25(4)	2	4 <sup>+</sup>	0.16(1)	8.0
1795.90(10)		(4 <sup>+</sup> , 3 <sup>-</sup> )	0.035(5)	8.5
1797.65(8)		(2 <sup>+</sup> , 1 <sup>-</sup> )	0.030(4)	8.4
1892.96(4)		(3,4) <sup>+</sup>	0.10(1)	7.6
1899.99(6)	2	2 <sup>+</sup>	0.070(6)	7.7
1906.78(12)		(2 <sup>+</sup> , 1 <sup>-</sup> )	0.041(5)	7.9
1928.53(8)		(3,4) <sup>+</sup>	0.053(5)	7.7
1937.17(10)		(3,4) <sup>+</sup>	0.067(6)	7.5
1944.85(3)	2	3 <sup>+</sup>	0.41(2)	6.6
1958.7(5)		2	0.0037(8)	8.6
1987.61(10)		4 <sup>+</sup>	0.042(4)	7.3
2010.17(4)	2	4 <sup>+</sup>	0.24(1)	6.2
2013.6(3)		(3,4) <sup>+</sup>	0.0032(9)	8.2
2022.73(9)		2 <sup>+</sup>	0.062(6)	6.8
2029.6(1)		(2 <sup>+</sup> )	0.021(3)	7.1
2037.0(2)		(3,4) <sup>+</sup>	0.007(1)	7.6
2123.1(3)		(2 <sup>+</sup> , 3 <sup>-</sup> )	0.0046(10)	5.6

## V. DISCUSSION

### A. Ground state rotational band: g.s.b.

From our precise  $\gamma$ -ray energy values, the improved level energies for the  $2^+$ ,  $4^+$ , and  $6^+$  states allowed us to calculate the rotational parameters  $A$ ,  $B$ , and  $C$  involved in the angular momentum expansion:

$$E_I = AI(I+1) + BI^2(I+1)^2 + CI^3(I+1)^3. \quad (1)$$

A comparison of calculated energies using  $A=9.766$  keV,  $B=24.0$  eV, and  $C=140$  meV with measured energies in the  $^{230}\text{Th}(\alpha, \alpha'2n\gamma)$  reaction,<sup>5</sup> exhibits significant discrepancies above spin  $I=8$ , meaning that  $^{228}\text{Th}$  is not a good rotor.

### B. The $K^\pi=0^-$ octupole band at 328.001(5) keV

This band is well known in  $^{228}\text{Th}$  up to spin  $I=5$  in the  $^{228}\text{Ac}$  and  $^{228}\text{Pa}$  decays from the Arbman *et al.*<sup>22</sup> and Dalmasso *et al.*<sup>11</sup> investigations; moreover, all states up to  $I=13$  are fed in the  $^{230}\text{Th}(\alpha, \alpha'2n\gamma)$  reaction.<sup>5</sup>

The reduced  $B(E1)$  transition probability ratios for the  $\gamma$  transitions deexciting the  $I=1, 3$ , and  $5$  states to members of the g.s. band,

$$B(E1; I^- \rightarrow I+1^+)/B(E1; I^- \rightarrow I-1^+)$$

are, respectively,  $1.99 \pm 0.17$ ,  $1.61 \pm 0.14$ , and  $1.57 \pm 0.26$

compared with 2.00, 1.33, and 1.2 for the squared Clebsch-Gordan coefficient ratios. The small deviations from the Alaga rule can be expressed by introducing the mixing parameter  $Z$  defined by<sup>23</sup>

$$Z = \langle 0^+ | M(E1, -1) | 1^- \rangle / \langle 0^+ | M(E1, 0) | 0^- \rangle. \quad (2)$$

Then the reduced  $B(E1)$  probability is given by<sup>23</sup>

$$B(E1; I_i \rightarrow I_f) = \langle K_f=0^+ | M(E1, 0) | K_i=0^- \rangle^2 \times \{ C(I_i, 0) \langle I_i 0 10 | I_f 0 \rangle + \sqrt{2} C(I_i, 1) \langle I_i 1 1-1 | I_f 0 \rangle Z \}^2, \quad (3)$$

where  $C(I_i, 0)$  and  $C(I_i, 1)$  are the admixed amplitudes of the  $K=0$  and  $1$  components in the representation

$$|IM\alpha\rangle = \sum_{K=0}^3 C(IK\alpha) |IMK\rangle, \quad (4)$$

where  $\alpha$ , omitted in formula (3), is generally taken as the  $K$  value of the main component. The  $B(E1)$  ratios calculated with our  $C(I, 0)$  amplitudes, deduced from a Coriolis coupling analysis (see Sec. VD), are in agreement with the experimental values using  $Z=2.3 \pm 1.0$ . Good agreement is also obtained between experimental energies and the calculated ones up to  $I=7$  with a Coriolis matrix element  $\langle 1^- | J^+ | 0^- \rangle = 0.31$  (Table IV, fit I).

TABLE IV. Level energies of the  $K^\pi=0^-, 1^-, 2^-$ , and  $3^-$  octupole bands in  $^{228}\text{Th}$ .

$K$	$I^\pi$	$E_{\text{exp}}$ (keV)	$E_{\text{calc}}^b$ (keV)	Fit I	$E_{\text{calc}}^c$ (keV)	Fit II
				Parameters <sup>d</sup> (keV)		Parameters <sup>d</sup> (keV)
0	$1^-$	328.00	328.0		328.0	
0	$3^-$	396.08	396.3		396.2	
0	$5^-$	519.20	519.1	$E_0 = 314.4$	519.1	$E_0 = 314.29$
0	$7^-$	695.4 <sup>a</sup>	696.4	$E_1 = 908.7$	696.7	$E_1 = 912.44$
0	$9^-$	921 <sup>a</sup>	928.4	$E_2 = 1106.4$	928.8	$E_2 = 1101.28$
0	$11^-$	1190 <sup>a</sup>	1214.9	$E_3 = 1316.3$	1215.6	$E_3 = 1315.91$
1	$1^-$		915.4	$A = 6.84$	919.3	$A = 6.83$
1	$2^-$	938.55	936.7		938.5	
1	$3^-$	969.38	969.0	$A_{1,0} = 2.3$	968.3	$A_{1,0} = -2.3 \times 10^{-4}$
1	$4^-$		1011.5	$A_{2,1} = 15.8$ $A_{3,2} = 14.5$	1009.2	$A_{2,1} = 18.8$ $A_{3,2} = 15.0$
2	$2^-$	1122.95	1123.1		1123.0	
2	$3^-$	1168.36	1168.9		1167.5	
2	$4^-$	1226.55	1226.0		1226.0	
2	$5^-$	1297.3	1297.4		1297.9	
3	$3^-$	1344.03	1344.0		1344.0	

<sup>a</sup>Experimental values measured in the  $^{230}\text{Th}(\alpha, \alpha'2n\gamma)$  reaction (Ref. 5).

<sup>b</sup>Calculated with the Coriolis interaction between four octupole bands and the adjusted parameter values  $E_K$ ,  $A_K$ , and  $A_{K+1,K}$  reported in the column 4.

<sup>c</sup>Calculated taking into account the Coriolis interaction between four octupole bands and the parameters  $E_K$ ,  $A_K$ , and  $A_{K+1,K}$  (column 6) deduced from the diagonalization procedure of Thomann and Piepenbring (Ref. 30).

<sup>d</sup> $E_K$ : band head energy involved in the unperturbed energy level [formula (10)];  $A_K$ : inertial parameter [formula (10)];  $A_{K+1,K}$ : Coriolis matrix element defined in formula (9).

### C. The $K^\pi=0^+$ band at 831.82(5) keV

An  $I^\pi=0^+$  level, previously found at 830 keV by Lederer,<sup>24</sup> and observed in the <sup>230</sup>Th(p,t) reaction<sup>4</sup> at  $E_x=830$  keV, is confirmed here by the strong coincidence of the 503.82-keV  $\gamma$  ray with the 270- and 328-keV energy gates. It depopulates also to the  $I^\pi=2^+$

$$B(E2;K2_2 \rightarrow 00_1):B(E2;K2_2 \rightarrow 02_1):B(E2;K2_2 \rightarrow 04_1) = 1:0.89(21):4.7(1.1);$$

this level is attributed  $K^\pi=0^+$  (the Alaga values are 1:1.42:2.57) and belongs to the  $K^\pi=0^+$  band at 831.82 keV. The inertial moment  $J_{0_2^+} = 70.3 \hbar^2 \text{ MeV}^{-1}$  is about 40% higher than that of the g.s. band ( $J_{0_1^+} = 51.3 \hbar^2 \text{ MeV}^{-1}$ ) and is close to that of the  $K^\pi=0^-$  octupole band ( $J_{0_-} = 73.6 \hbar^2 \text{ MeV}^{-1}$ ). Such a characteristic strongly supports the idea that this excitation contains two octupole phonons as the main component. Although the theoretical energy of such an excitation should be  $\sim 630$  keV, the multiphonon method, developed by Piepenbring,<sup>25</sup> predicts that it should be strongly anharmonic and pushed up in energy. Microscopic calculations from Ivanova *et al.*<sup>26</sup> predict an 83% squared amplitude for two octupole phonon composition in this  $0_2^+$  state.

This band might also be interpreted as the  $1\alpha$  band predicted by the nuclear vibron model (NVM).<sup>2,3</sup> In this model, a sensitive parameter is the reduced hindrance factor (RHF) given by<sup>2,27</sup>

$$\text{RHF} = \tan^2(\theta_2/2) = \frac{B(E1;2_\alpha^+ \rightarrow 3_1^-)}{B(E1;2_1^+ \rightarrow 3_1^-)} \approx 10, \quad (5)$$

where  $\theta_2$ , the mixing angle for  $0\alpha$  plus  $1\alpha$  mixing,<sup>2</sup> is parameter-free and only based on the  $\alpha$ -decay data.

From our intensity values, we can calculate the reduced  $B(E1)/B(E2)$  ratio for the  $2^+$  member of the  $K^\pi=0_2^+$  band using

$$\begin{aligned} \frac{B(E1;0_22^+ \rightarrow 3_1^-)}{B(E2;0_22^+ \rightarrow 4_1^+)} &= \frac{I_\gamma(E1)E_\gamma^5(E2) \times 0.03}{I_\gamma(E2)E_\gamma^3(E1) \times (197.1)^2} \\ &= 3.4 \times 10^{-6} \text{ fm}^{-2}, \end{aligned} \quad (6)$$

where the  $E_\gamma$  are in MeV (the mean value for all the members of the  $K^\pi=0_2^+$  is  $7.6 \times 10^{-6} \text{ fm}^{-2}$ ). Dividing by the reduced ratio value

$$B(E1;3_1^- \rightarrow 2_1^+)/B(E2;3_1^- \rightarrow 1_1^-) \approx 10^{-8} \text{ fm}^{-2},$$

estimated from the experimental systematics,<sup>27,28</sup> led us, after rearranging, to

$$\frac{B(E1;0_22^+ \rightarrow 3_1^-)}{B(E1;0_12^+ \rightarrow 3_1^-)} \frac{7}{5} \frac{B(E2;3_1^- \rightarrow 1_1^-)}{B(E2;0_22^+ \rightarrow 0_14^+)} \approx 3.4 \times 10^2. \quad (7)$$

Assuming

member of the g.s. band by a 774.1-keV  $\gamma$  transition. An 874.44-keV state, not found in the <sup>228</sup>Pa decay, is observed here to decay to  $I^\pi=0^+$ ,  $2^+$ , and  $4^+$  members of the g.s. band, and to  $I^\pi=1^-$ ,  $3^-$  of the  $K^\pi=0^-$  octupole band. This decay pattern leads to a unique assignment of  $I^\pi=2^+$ , in agreement with the value  $I=2$  found in the <sup>230</sup>Th(p,t) experiment<sup>4</sup> for the 874-keV level. From reduced  $B(E2)$  considerations,

$$\frac{7}{5} B(E2;3_1^- \rightarrow 1_1^-) \approx B(E2;0_12^+ \rightarrow 0_10^+),$$

we can evaluate the ratio

$$B(E2;0_22^+ \rightarrow 0_14^+)/B(E2;0_12^+ \rightarrow 0_10^+) = 2.8 \times 10^{-2}$$

by using our  $B(E2)$  ratios

$$B(E2;0_22^+ \rightarrow 0_14^+)/B(E2;0_22^+ \rightarrow 0_12^+) = 4.7,$$

and the value

$$B(E2;0_22^+ \rightarrow 0_12^+)/B(E2;0_12^+ \rightarrow 0_10^+) \approx 6 \times 10^{-3}$$

measured in the <sup>230</sup>Th nucleus.<sup>29</sup> We can deduce

$$B(E1;0_22^+ \rightarrow 3_1^-)/B(E1;0_12^+ \rightarrow 3_1^-) \approx 9.5.$$

In spite of the crude approximations used here, this ratio is in good agreement with the theoretical prediction of the NVM [Eq. (5)]. However, experimental data of our work are not sufficient to discriminate between the two interpretations given above.

### D. Possible $K^\pi=1^-$ octupole band

A  $K^\pi=1^-$  band was tentatively identified in <sup>228</sup>Th from the <sup>228</sup>Pa decay study by Kurcewicz *et al.*,<sup>6</sup> with the states  $I=1, 2, 3$ , and  $4$  having the respective energies 951.9, 969, 1015.6, and 1064.1 keV. However, in our <sup>228</sup>Ac decay scheme (Fig. 4), the  $I=1$  and  $4$  are not fed. We assign the spin  $I^\pi=2^+$  to the 1016.42-keV level, because of its decay to the  $0^+$  g.s. Moreover, a 968.38-keV state, newly reported in the <sup>228</sup>Ac decay, mainly deexcites to  $I=1, 3$ , and  $5$  members of the  $K^\pi=0^-$  octupole band. Such decay characteristics are consistent with an  $I=3$  assignment and a negative parity. Furthermore, a new 938.5-keV level, based on good energy fits of the 880.76- and 610.64-keV  $\gamma$  rays to respective  $2^+$  g.s. and  $KI^\pi=01^-$  states, might be an  $I^\pi=2^-$  candidate (although  $I^\pi=0^+$  cannot be excluded). This hypothesis allowed us to deduce for this tentative  $K^\pi=1^-$  band an inertial parameter  $A = -\hbar^2/2J = 4.99 \text{ keV}$ , a value which is not in disagreement with analogous values calculated in nearby nuclei <sup>230</sup>Th (Ref. 29) or <sup>234</sup>U (Ref. 15).

A Coriolis coupling analysis has been performed including the four octupole bands  $K^\pi=0^-$ ,  $1^-$ ,  $2^-$ , and  $3^-$ . This analysis took into account the energies of the  $I=1, 3$ , and  $5$  members of the  $K^\pi=0^-$  band, the  $I=2$  and  $3$  members of the  $K^\pi=1^-$  band, and the  $I=2, 3$ , and  $4$  members of the  $K^\pi=2^-$  band. For the  $K^\pi=3^-$

band, two levels at 1344.03 and 1450.29 keV are candidates. The energy of the first one was introduced in the fits, but such a choice does not strongly modify the conclusion of this analysis. In the calculation, the off-diagonal matrix elements are taken equal to

$$\langle K+1, I | H_c | K, I \rangle = A_{K+1, K} [(1 + \delta_{K,0})(I-K)(I+K+1)]^{1/2}, \quad (8)$$

with

$$A_{K+1, K} = -(\hbar^2/2J)_c \langle K+1 | J_+ | K \rangle. \quad (9)$$

In Fit I the  $A_{K+1, K}$  were treated as adjustable parameters along with the inertial parameter  $A_K$  involved in the diagonal matrix element describing the unperturbed level energies

$$E_{IK} = E_K + A_K [I(I+1) - K^2]. \quad (10)$$

Moreover, the  $A_K$  were assumed to be equal for all the bands involved. In Fit II the matrix diagonalization was performed using a computer code described by Thomann and Piepenbring.<sup>30</sup> Experimental level energies of the  $K^\pi = 0^-, 1^-,$  and  $2^-$  bands are well reproduced up to

$$B(E2; 2I_i \rightarrow 0I_f) = \langle 2I_i 2-2 | I_f 0 \rangle^2 M^2 \{1 + a_\gamma [I_f(I_f+1) - I_i(I_i+1)]\}^2 \quad (11)$$

lead to nonoverlapping values of the mixing parameter  $a_\gamma$ . This disagreement can be interpreted as due to a non-negligible coupling with the  $K^\pi = 0_2^+$  ( $1\alpha$  band) at 831.82 keV. The introduction of the coupling  $Z_{\beta\gamma}$  with this band by means of the formula

$$B(E2; 2I_i \rightarrow 0I_f) = \langle 2I_i 2-2 | I_f 0 \rangle^2 M^2 [1 + Z_\gamma F_\gamma(I_i, I_f) + Z_{\beta\gamma} F_{\beta\gamma}(I_i, I_f)]^2, \quad (12)$$

where the  $F_\gamma(I_i, I_f)$  and  $F_{\beta\gamma}(I_i, I_f)$  have been tabulated by Riedinger *et al.*,<sup>32</sup> gives the values  $\bar{Z}_\gamma = (36 \pm 6) \times 10^{-3}$  and  $Z_{\beta\gamma} = -(28 \pm 5) \times 10^{-3}$ . This  $\bar{Z}_\gamma$  value overlaps the value  $Z_\gamma = (39 \pm 4) \times 10^{-3}$  obtained for the  $KI^\pi = 23^+$  level which is uncoupled from the  $1\alpha$  band.

#### F. The 979.50(3)-keV level

This new reported level deexcited mainly to  $I=0^+$ ,  $2^+$  members of the g.s. band and to  $I^\pi = 1^-, 3^-$  levels of the octupole band. The most probable character is then  $I^\pi = 2^+$  and it seems possible to identify this level with the  $I^\pi = 2^+$  state observed in the  $^{230}\text{Th}(p,t)$  reaction<sup>4</sup> at  $E_x = 977 \pm 5$  keV. No strong argument is available to distinguish between  $K=0$  or  $2$  for this level.

#### G. The $K^\pi = 2^-$ band at 1122.945(8) keV

This third octupole band was previously found up to  $I=4$  in both  $^{228}\text{Ac}$  (Refs. 7 and 11) and  $^{228}\text{Pa}$  (Ref. 6) decays. Four new interband transitions are placed to the "γ band," at 77.34, 100.41, 135.54, and 257.2 keV. The  $I^\pi = 5^-$  state is identified here at 1297.31 keV because of the coincidence of the 901.2-keV γ line with the 338-keV gate; furthermore, its energy value agrees fairly well with the value  $E_5 = 1293$  keV, calculated using the rotational

spin  $I=7$  ( $K^\pi = 0^-$ ) within 1.5 keV by Fit I and Fit II (Table IV). However, the smallness of the  $\langle 1^- | J_+ | 0^- \rangle$  matrix element ( $-3.4 \times 10^{-5}$ ) found in Fit II might imply a complete decoupling of the  $K^\pi = 0^-$  and  $1^-$  bands. Such a situation would not agree with the observation of small deviations in the  $B(E1)$  ratios from the  $K^\pi = 0^-$  band (see Sec. VB). Also, the value  $\langle 1^- | J_+ | 0^- \rangle = 0.31$  given in Fit I, which is of the same order of magnitude as that in  $^{230}\text{Th}$  (Ref. 29) was preferred.

#### E. The $K^\pi = 2^+$ band at 968.973(8) keV

The so-called γ band in  $^{228}\text{Th}$  has been well known since the Arbman *et al.*<sup>22</sup> work. The states with  $I=2, 3,$  and  $4$  are at respective energies of 968.973, 1022.52, and 1091.00 keV. Using the  $E_0, A,$  and  $B$  parameters fitted from these three members, the  $I^\pi = 5^+$  state is predicted to have an energy of 1171.9 keV. The 1174.52 keV level, based on a single γ transition of 987.7 keV feeding the  $4^+$  level, can be identified with it and is quite different from the 1175.41-keV ( $I^\pi = 2^+$ ) level.

Reduced  $B(E2)$  and  $B(M1)$  ratios to the g.s. band calculated for each member of the γ band using the Mikhailov formula<sup>31</sup>

formula with two inertial parameters. From the energies of the four members of this  $K=2$  band and the formula<sup>33</sup>

$$E_I = E_0 + AI(I+1) + BI^2(I+1)^2 + (-1)^{I+1} A_4(I-1)I(I+1)(I+2) \quad (13)$$

we deduce  $A = 9.274$  keV,  $B = -20.6$  eV, and  $A_4 = -0.90$  eV. A small signature splitting can be inferred from this  $A_4$  value, comparable to that observed in the  $^{234}\text{U}$  nucleus (i.e.,  $A_4 = -0.68$  eV).<sup>15</sup> Besides, in the Coriolis analysis described above (Sec. VD and Table IV), the energy values of the  $I=2-5$  members of this  $K^\pi = 2^-$  band are well reproduced using the values  $\langle 2^- | J_+ | 1^- \rangle = 2.31$  for the Coriolis matrix element and  $A = 6.82$  keV as the single inertial parameter for the four octupole bands.

#### H. The 1153.49(2)-keV level

This  $I^\pi = 2^+$  level was reported earlier in the  $^{228}\text{Ac}$  (Refs. 7 and 11) and  $^{228}\text{Pa}$  (Ref. 6) decays. An additional transition was found to the 979-keV ( $I^\pi = 2^+$ ) level. The reduced transition probability ratios to the g.s. members are consistent either with a  $K=0$  or  $2$  assignment; however, considering the reduced transition probability ratios to g.s. band members versus those of the  $K^\pi = 0_2^+$  or of the  $K^\pi = 2^+$  bands, i.e.,

$$B(E2;K2^+ \rightarrow 0_1 2^+)/B(E2;K2^+ \rightarrow 0_2 2^+) \\ = (7.2 \pm 0.8) \times 10^{-3},$$

and

$$B(E2;K2^+ \rightarrow 0_1 2^+)/B(E2;K2^+ \rightarrow 22^+) \\ = (2.7 \pm 0.4) \times 10^{-4},$$

we notice a strong enhancement of the transition strength to the one-phonon band and to the  $1\alpha$  ( $K^\pi=0_2^+$ ) band (in the sense of the NVM, Refs. 2 and 3). Such a characteristic can be interpreted as evidence for a highly anharmonic two-quadrupole phonon state for which examples are found in <sup>234</sup>U (Ref. 15) and <sup>230</sup>Th (Ref. 29) nuclei. In the framework of the NVM (Ref. 3), this level is considered as the  $\gamma$  band of the  $1\alpha$  configuration.

#### I. The 1175.41(6)-keV level

This level was not found in <sup>228</sup>Pa decay and was suggested in <sup>228</sup>Ac decay as a  $2^+$  level. This assignment is confirmed here because it decays to  $I^\pi=0^+$ ,  $2^+$ , and  $4^+$  members of the g.s. band and to the 944.18 keV ( $I^\pi=2^+$ ) level.

#### J. The 1344.03(9)-keV level

This level was suggested to be fed in <sup>228</sup>Ac decay,<sup>7</sup> but not in <sup>228</sup>Pa decay.<sup>6</sup> Additional  $\gamma$  lines found at 1286.7, 1157.14, and 168.65 keV are interpreted here as deexciting to  $2^+$ ,  $4^+$ , and to the  $I^\pi=2^+$  level at 1175.41 keV. It deexcites also to  $I^\pi=1^-$ ,  $3^-$ , and  $5^-$  members of the octupole band, and should have a spin  $I^\pi=3^-$ . This state might be the first  $K^\pi=3^-$  octupole state expected at 1.5 MeV from the calculations of Soloviev and Siklos,<sup>34</sup> having the two quasineutron structure

$$\left\{ \frac{3}{2}^-(761)_n + \frac{3}{2}^+(631)_n \right\}_{K^\pi=3^-}$$

It could be populated from the <sup>228</sup>Ac ground state for which the two-quasiparticle configuration

$$\left\{ \frac{3}{2}^+(631)_n + \frac{3}{2}^+(651)_p \right\}_{K^\pi=3^+}$$

is assumed.<sup>22</sup>

#### K. The 1431.98(1)-keV level

This level decays mainly to the first three excited states of the  $K^\pi=2^+$  “ $\gamma$  band” by well known  $E2$  and  $M1$  transitions. Additional  $\gamma$  lines at 452.47 and 1103.41 keV are interpreted as deexciting it to the  $I^\pi=2^+$  level at 979.50 keV and to the  $KI^\pi=01^-$  level. The existence of this last transition adds evidence for the assignment  $KI^\pi=33^+$ , instead of  $KI^\pi=44^+$  as proposed by Kurcewicz *et al.*<sup>6</sup> Furthermore, the reduced probability ratio to the “ $\gamma$  band,”

$$B(E2;33^+ \rightarrow 22^+)/B(E2;33^+ \rightarrow 23^+) = 1.21 \pm 0.09,$$

agrees well with the theoretical value, i.e., 0.85 for  $K=3$ , and leads to the mixing parameter value  $a = -(0.031 \pm 0.007)$ . As regards its quasiparticle

configuration, neither the two quasiproton state

$$\left\{ \frac{5}{2}^-(523)_p + \frac{1}{2}^-(530)_p \right\}_{K^\pi=3^+}$$

expected at 2.0 MeV by the calculations of Soloviev and Siklos,<sup>34</sup> nor the quasineutron states

$$\left\{ \frac{5}{2}^-(752)_n + \frac{1}{2}^-(770)_n \right\}_{K^\pi=3^+}$$

or

$$\left\{ \frac{5}{2}^-(752)_n + \frac{1}{2}^-(501)_n \right\}_{K^\pi=3^+}$$

calculated by Blocki and Kurcewicz<sup>35</sup> can be fed by <sup>228</sup>Ac  $\beta$  decay according to the one-particle selection rule;<sup>36</sup> however, the two-quasiproton configuration

$$\left\{ \frac{3}{2}^+(402)_p + \frac{3}{2}^+(651)_p \right\}_{K^\pi=3^+}$$

might describe the 1432.0 keV state structure. The related neutron transition

$$\frac{3}{2}^+(631)_n \rightarrow \frac{3}{2}^+(402)_p$$

( $\Delta N=2, \Delta n_z=3$ ) is typically a  $1h\beta$  transition with high  $\log ft$  value. We obtain  $\log ft=7.9$ .

#### L. The $K^\pi=2^+$ band at 1638.23(3) keV

The spin value  $I=2$  is assigned to the 1638.23-keV state, depopulating to  $I=0, 2$ , and  $4$  members of the g.s. band and to the octupole state  $KI^\pi=01^-$ . The  $K=2$  character seems to be the most likely, from reduced  $B(E2)$  ratios. A 1688.38-keV level is established, decaying to  $I=2$  and  $4$  members of the g.s. band, to the  $KI^\pi=0_2 2^+$  state, and to the  $I^\pi=2^+$  state at 1016.42 keV. Although the assignment  $I=4$  cannot be excluded, the lack of deexcitation to the  $I^\pi=6^+$  level of the g.s. band favors a spin value  $I=3$ . We thus tentatively assign these levels as the two first excited states of a  $K=2$  rotational band, for which the inertial parameter value  $A=8.36$  keV was deduced. The third excited state of this band,  $I^\pi=4^+$ , might be the 1760.25 keV level, decaying to the  $I^\pi=2^+$  and  $4^+$  states of the g.s. band, to the  $I^\pi=2^+$  and  $3^+$  states of the “ $\gamma$  band,” and to the  $I^\pi=4^-$  state of the  $K^\pi=2^-$  octupole band. The energy fits the  $I(I+1)$  law well. Moreover, allowing for  $I=3$  for the <sup>228</sup>Ac ground state,<sup>22</sup> the  $ft$  ratio of the  $\beta$  transitions to these  $I^\pi=3^+$  and  $4^+$  states agrees fairly well with the Alaga values, i.e.,

$$\frac{ft(33^+ \rightarrow 24^+)}{ft(33^+ \rightarrow 23^+)} = 6.46 \pm 0.50,$$

compared with

$$(\langle 3311 | 32 \rangle / \langle 3311 | 42 \rangle)^2 = 6.94.$$

With regard to the two-quasiparticle structure of these  $K^\pi=2^+$  states, the two-proton configurations<sup>34</sup>

$$\left\{ \frac{5}{2}^-(532)_p - \frac{1}{2}^-(530)_p \right\}_{K^\pi=2^+}$$

and

$$\left\{ \frac{5}{2}^-(523)_p - \frac{1}{2}^-(530)_p \right\}_{K^\pi=2^+},$$



with respective energies of 1.8 and 2.0 MeV, cannot be fed by  $^{228}\text{Ac}$  decay, by virtue of the  $F$ -selection rule.<sup>36</sup> The investigation of the Nilsson states available for a deformation parameter<sup>37</sup>  $\nu_2=0.2$  suggests possible two-quasiproton configurations:

$$(I) \left\{ \frac{3}{2}^+(651)_p + \frac{1}{2}^+(660)_p \right\}_{K^\pi=2^+}$$

or

$$(II) \left\{ \frac{3}{2}^+(651)_p + \frac{1}{2}^+(400)_p \right\}_{K^\pi=2^+}.$$

Configuration (I) seems preferable to describe this  $K^\pi=2^+$  state because the  $\beta$  transition involved,  $\frac{3}{2}^+(631)_n \rightarrow \frac{1}{2}^+(660)_p$  ( $\Delta N=0$ ,  $\Delta n_z=3$ ,  $\Delta \Lambda=0$ ), is less hindered than the corresponding transition to the  $\frac{1}{2}^+(400)_p$  orbital ( $\Delta N=2$ ). However, a quasiproton configuration including the  $\frac{1}{2}^+(400)_p$  orbital might be fed by  $\beta$  decay, if we assume that the  $^{228}\text{Ac}$  ground state contains a small

$$\left\{ \left( \frac{5}{2}^+(633)_n + \frac{1}{2}^+(400)_p \right) \right\}_{K^\pi=3^+}$$

admixture in its wave function.

#### M. The $K^\pi=2^+$ band at 1899.99 keV

From the same type of arguments developed above, a  $K^\pi=2^+$  band was built involving  $I^\pi=2^+$ ,  $3^+$ , and  $4^+$  levels at respective energies of 1899.99(6), 1944.85(3), and 2010.17(4) keV (Fig. 4).

The 1899.99-keV level is limited to the spin value  $I^\pi=2^+$  since it decays to  $0^+$ ,  $2^+$ , and  $4^+$  members of the g.s. band, and to  $I^\pi=3^+$  of the " $\gamma$  band." The 1944.85 keV state deexcites to the  $I=2, 4$  levels of the g.s. band and to  $I=2, 4$  levels of the " $\gamma$  band," to  $I^\pi=2^+$  levels at 944.18 and 1175.41 keV and to the  $I=4$  member of the  $K^\pi=2^-$  octupole band. Reduced  $B(E2)$  transition probability ratios from this level to members of the g.s. band agree well with the assignment  $KI^\pi=23^+$ . The inertial parameter value  $A=7.48$  keV, deduced from the energy separation of these two levels, led us to estimate the position of the  $I^\pi=4^+$  member of this band to be 2004.6 keV. The well-established 2010.17 keV level, which mainly decays to  $I=2, 3$ , and  $4$  members of the g.s. band and to  $I^\pi=2^+, 4^+$  members of the  $\gamma$  band, seems to be a good candidate for the  $4^+$  state of this last band. The quasiparticle structure of

this  $K^\pi=2^+$  band might also be represented by either configuration (I) or (II), but no strong argument can be given for any of these interpretations.

#### N. Other levels

Twenty-six additional levels were proposed (Fig. 4) between 1416 and 2123 keV based essentially on good energy sums of at least (with four exceptions) three  $\gamma$  rays deexciting each of them. Their tentative spin and parity were assigned based on their deexcitation modes and the  $\beta$  decay selection rules.

## VI. CONCLUSION

In summary, this study led us to place more than 225  $\gamma$  lines from  $^{228}\text{Ac}$  decay among 58 excited levels in  $^{228}\text{Th}$ . The analysis of Coriolis coupling between four octupole bands in  $^{228}\text{Th}$ ,  $K^\pi=0^-, 1^-, 2^-, 3^-$ , was carried out. The  $K^\pi=0^-$  band is weakly coupled to a possible  $K^\pi=1^-$  band, for which the  $I=2$  and  $3$  members were located at 938.5 and 968.38 keV. The  $K^\pi=2^-$  band was found to be fed up to spin  $I=5$ . As concerns the  $K^\pi=3^-$  states, a new  $I^\pi=3^-$  level at 1344.03 keV was observed in addition to the known 1450.29 keV ( $KI^\pi=33^-$ ). The  $K^\pi=0_2^+$  band at 831.82 keV cannot be described as a " $\beta$  band," as has been demonstrated in the two-neutron transfer reactions.<sup>4</sup> It seems possible to interpret its preferential decay to the octupole band as characteristic of a two octupole phonon composition; however, this excitation might correspond to the  $1\alpha$  band predicted by the NVM of Daley and Iachello.<sup>3</sup> Several other  $I^\pi=2^+$  states built at 944.18, 979.50, 1016.41, 1175.41, and 1415.92 keV might be attributed  $K^\pi=0^+$ ; however, no explanation can be given on the nature (collective or intrinsic) of these low energy  $2^+$  states.

## ACKNOWLEDGMENTS

We wish to thank Dr. R. Piepenbring of the Institut des Sciences Nucléaires de Grenoble for providing his computer code and for valuable discussions. We are gratefully indebted to Dr. Henry J. Daley of the Daresbury Laboratory for his illuminating comments and suggestions about the theoretical interpretation of experimental data.

<sup>1</sup>H. Daley and F. Iachello, Phys. Lett. **131B**, 281 (1983).

<sup>2</sup>H. J. Daley and B. R. Barrett, Nucl. Phys. **A449**, 256 (1986).

<sup>3</sup>H. J. Daley and F. Iachello, Ann. Phys. (N.Y.) **167**, 73 (1986).

<sup>4</sup>J. V. Maher, J. R. Erskine, A. M. Friedman, J. P. Schiffer, and R. H. Siemssen, Phys. Rev. Lett. **25**, 302 (1970); J. V. Maher, J. R. Erskine, A. M. Friedman, R. H. Siemssen, and J. P. Schiffer, Phys. Rev. C **5**, 1380 (1972).

<sup>5</sup>K. Hardt, P. Schuler, C. Gunther, J. Recht, K. P. Blume, and H. Wilzek, Nucl. Phys. **A419**, 34 (1984).

<sup>6</sup>W. Kurcewicz, K. Stryczniewicz, J. Zylicz, R. Broda, S. Chojnacki, W. Walus, and I. Yutlandov, J. Phys. (Paris) **34**, 159 (1973).

<sup>7</sup>M. Herment and C. Vieu, C. R. Acad. Sci. **273B**, 1058 (1971).

<sup>8</sup>M. Herment, A. Peghaire, C. F. Leang, C. R. Acad. Sci. Paris **273B**, 801 (1971).

<sup>9</sup>J. Dalmaso and H. Maria, C. R. Acad. Sci. Paris **272B**, 905 (1971).

<sup>10</sup>J. Dalmaso and H. Maria, C. R. Acad. Sci. Paris **273B**, 568 (1971).

<sup>11</sup>J. Dalmaso, H. Maria, and C. Ythier, C. R. Acad. Sci. Paris **278B**, 97 (1974).

<sup>12</sup>D. J. Horen, Nucl. Data Sheets **17**, 367 (1976).

<sup>13</sup>J. Dalmaso, H. Maria, A. Hachem, G. Barci, and G. Ardisson, J. Radioanal. Nucl. Chem. Lett. **86**, 53 (1984).

- <sup>14</sup>R. G. Helmer, Nucl. Instrum. Methods **164**, 355 (1979).
- <sup>15</sup>C. Ardisson, J. Dalmasso, and G. Ardisson, Phys. Rev. C **33**, 2132 (1986).
- <sup>16</sup>S. K. Bhattacharjee, S. K. Mitra, H. C. Jain, H. C. Padhi, K. S. Bhatki, and D. C. Ephraim, Nucl. Phys. **A90**, 696 (1967).
- <sup>17</sup>F. Rösler, H. M. Fries, K. Adler, and H. C. Pauli, At. Data Nucl. Data Tables **21**, 292 (1978).
- <sup>18</sup>A. H. Wapstra and G. Audi, Nucl. Phys. **A432**, 1 (1985).
- <sup>19</sup>G. Skarnemark and M. Skalberg, Int. J. Appl. Radiat. Isot. **36**, 439 (1985).
- <sup>20</sup>N. B. Gove and M. J. Martin, Nucl. Data Tables **10**, 206 (1971).
- <sup>21</sup>U. Schötzig and K. Debertin, Int. J. Appl. Radiat. Isot. **34**, 533 (1983).
- <sup>22</sup>E. Arberman, S. Bjørnholm, and O. B. Nielsen, Nucl. Phys. **21**, 406 (1960).
- <sup>23</sup>L. Kocbach and P. Vogel, Phys. Lett. **32B**, 434 (1970).
- <sup>24</sup>C. M. Lederer, thesis, University of California Radiation Laboratory, 1963, University of California Radiation Laboratory Report 11028, 1963.
- <sup>25</sup>R. Piepenbring, Phys. Rev. C **27**, 2968 (1983).
- <sup>26</sup>S. P. Ivanova, A. L. Komov, L. A. Malov, and V. G. Soloviev, Fiz. Elem. Chastits At. Yadra **7**, 450 (1976) [Sov. J. Part. Nucl. **7**, 175 (1976)].
- <sup>27</sup>H. J. Daley, private communication.
- <sup>28</sup>M. Gai, in *Proceedings of the Conference on Nuclear Structure with Heavy Ions, Legnaro, Italy, 1985*, edited by R. A. Ricci and C. Villi (Editrice Compositore, Bologna, 1986), Vol. 2, p. 20.
- <sup>29</sup>J. Gerl, Th. W. Elze, H. Ower, H. Bohn, T. Faestermann, N. Kaffrell, and N. Trautmann, Phys. Rev. C **29**, 1684 (1984).
- <sup>30</sup>J. Thomann and R. Piepenbring, J. Phys. (Paris) **33**, 613 (1972).
- <sup>31</sup>V. M. Mikhailov, Izv. Akad. Nauk SSSR, Ser. Fiz. **30**, 1334 (1966).
- <sup>32</sup>L. L. Riedinger, N. R. Johnson, and J. H. Hamilton, Phys. Rev. **179**, 1214 (1969).
- <sup>33</sup>A. Bohr and B. R. Mottelson, *Nuclear Structure* (Benjamin, New York, 1975), Vol. 2.
- <sup>34</sup>V. G. Soloviev and T. Siklos, Nucl. Phys. **59**, 145 (1964).
- <sup>35</sup>J. Blocki and W. Kurcewicz, Phys. Lett. **30B**, 458 (1969).
- <sup>36</sup>V. G. Soloviev, Nucl. Phys. **A69**, 1 (1965).
- <sup>37</sup>R. R. Chasman, I. Ahmad, A. M. Friedman, and J. R. Erskine, Rev. Mod. Phys. **49**, 833 (1977).